Electronic Supplementary Material (ESI) for Journal of Materials Chemistry B.


**Supplementary Information**

# Enzymatic Synthesis of PEG-poly(amine-*co*-thioether esters) as Highly Efficient pH and ROS Dual-Responsive Nanocarriers for Anticancer Drug Delivery

Yi-hong Gong[a,1], Man Shu[a,1], Jian-hua Xie[a,], Chao Zhang[a], Zhong Cao[a], Zhao-zhong Jiang[b,*], Jie Liu[a,*]

[a] *School of Biomedical Engineering, Sun Yat-sen University, Guangzhou, Guangdong 510275, China*

[b] *Department of Biomedical Engineering, Integrated Science and Technology Center, Yale University, 600 West Campus Drive, West Haven, Connecticut 06516, United States*

[1] These authors contribute equally to this work.

* To whom correspondence may be addressed. E-mail: liujie56@mail.sysu.edu.cn or zhaozhong.jiang@yale.edu

# Supplementary Information

## 1. Structural characterization of PEG-PPMT block copolymers

The molecular structures of PEG-PPMT copolymers were analyzed by $^{1}H$ and $^{13}C$ NMR spectroscopy. The assignments of NMR resonance absorptions were assisted by observing the variations in peak intensity vs the polymer composition. Figure S1 shows structural assignments for the proton resonance absorbances and major carbon-13 absorbances of PEG-PPMT copolymers. Further, the carbonyl groups of the polymers exhibited four carbon-13 resonances at 171.66, 171.80, 173.69 and 173.89 ppm corresponding respectively to TDP*-MDEA, TDP*-PDL, PDL*-MDEA and PDL*-PDL diads in the polymer chains (Figure S2-A). The abundances of the four diads were

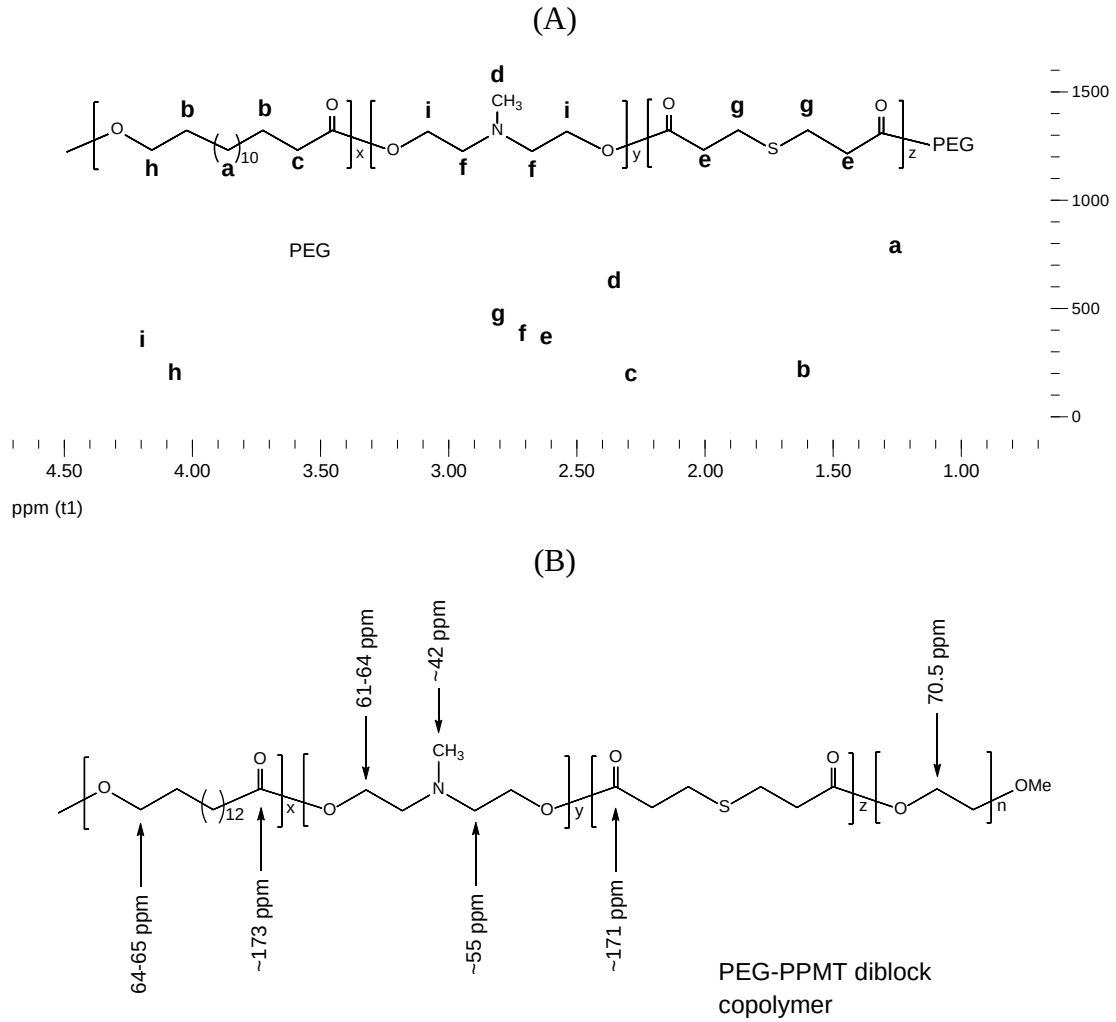


**Figure S1**. Structural assignments for the proton NMR resonance absorptions (A) and major carbon-13 resonance absorptions (B) of PEG-PPMT copolymers. The proton NMR spectrum in A corresponds to PEG-PPMT-40% PDL.

quantitatively measured for PEG-PPMT-40% PDL and PEG-PPMT-70% PDL, and were compared to the values calculated for random PPMT chains at the same compositions (Figure S2-B). The results indicate that the distributions of PDL, MDEA, and TDP repeat units in the copolymer PPMT chain segments are near statistically random.

(A)

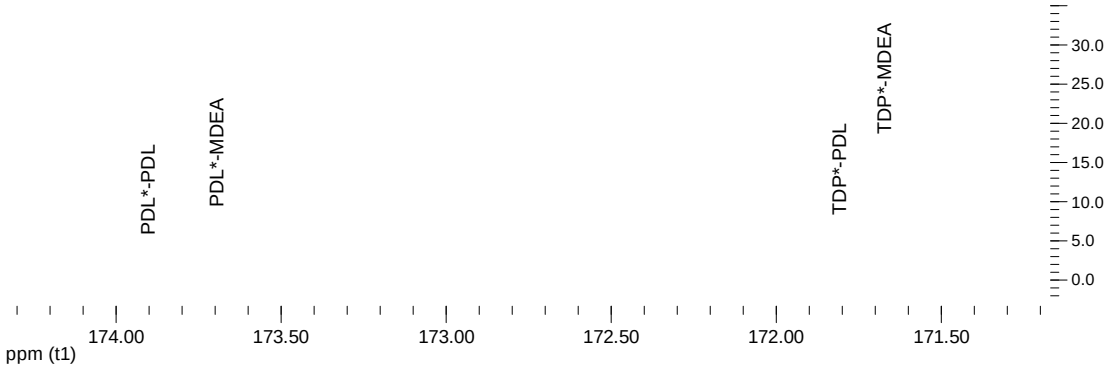


(B)

| Sample | PDL*-PDL | | PDL*-MDEA | | TDP*-PDL | | TDP*-MDEA | |
|---|---|---|---|---|---|---|---|---|
| | Meas. [a] | Calc. [b] | Meas. [a] | Calc. [b] | Meas. [a] | Calc. [b] | Meas. [a] | Calc. [b] |
| PEG-PPMT-40% PDL | 0.08 | 0.06 | 0.19 | 0.19 | 0.19 | 0.19 | 0.54 | 0.56 |
| PEG-PPMT-70% PDL | 0.31 | 0.29 | 0.24 | 0.25 | 0.24 | 0.25 | 0.20 | 0.21 |

a. Measured by carbon-13 NMR spectroscopy.

b. Calculated for random poly(PDL-*co*-MDEA-*co*-TDP) chains. Abundance of PDL*-PDL = $f_P \times f_P$ ; abundance of PDL*-MDEA = $f_P \times (2 \times f_M)$; abundance of TDP*-PDL = $(2 \times f_T) \times f_P$ ; abundance of TDP*-MDEA = $(2 \times f_T) \times (2 \times f_M)$. The symbols $f_P$, $f_M$ and $f_T$ represent respectively molar fractions of PDL, MDEA and TDP units in the copolymer chains.

**Figure S2**. Carbonyl C-13 resonance absorbances of different diads in PEG-PPMT-40% PDL (A) and diad distributions in PEG-PPMT copolymer chains (B).

(A)

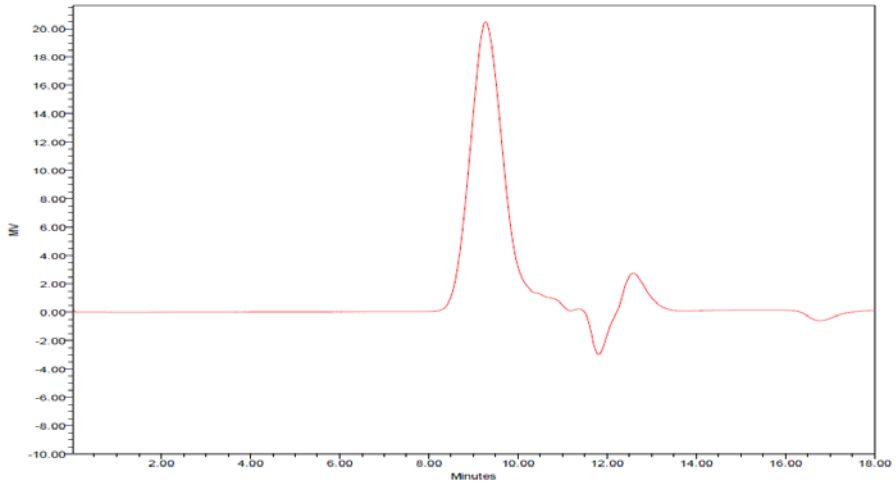


(B)

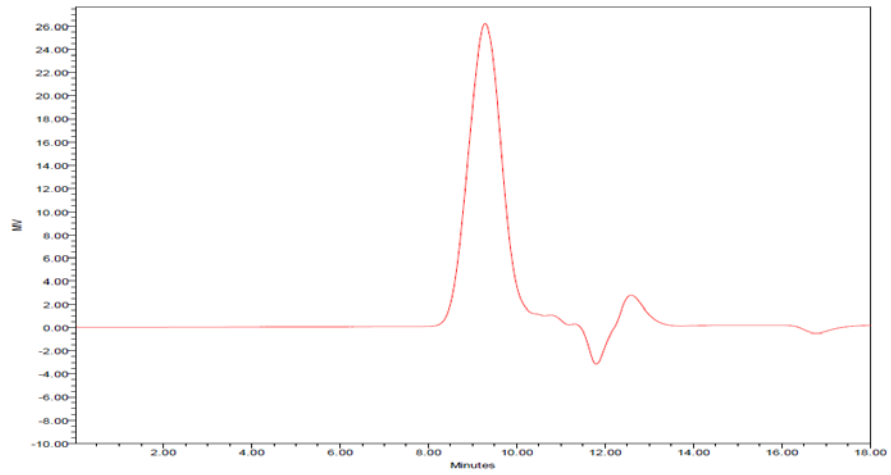


(C)

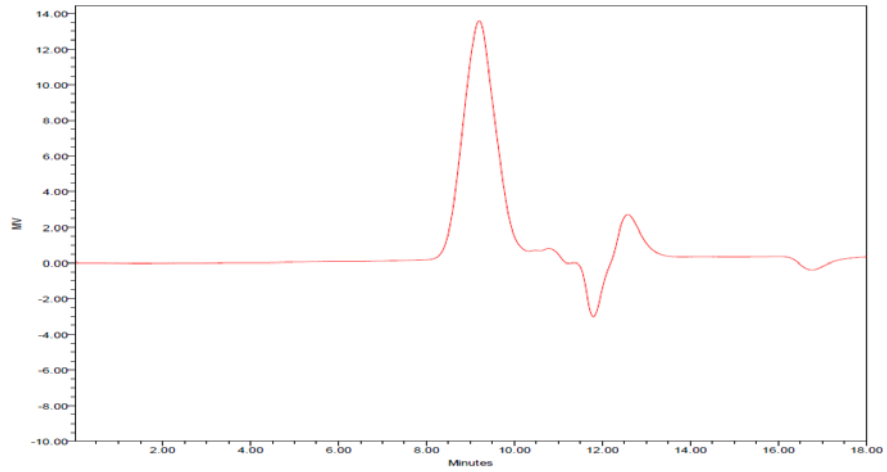


**Figure S3.** GPC traces of (A) PEG-PPMT-11% PDL, (B) PEG-PPMT-28% PDL, and (C) PEG-PPMT-40% PDL. The signals after the polymer peaks (11-14 min) are due to injection noises.

## 2. Critical micelle concentration (CMC) measurement

The critical micelle concentration (CMC) values of PEG-PPMT copolymers were measured by fluorescence spectroscopy using pyrene as a probe molecule according to previously reported procedures.[S1] The CMC value was estimated as the nanoparticle concentration at the cross point in the curves of $I_3/I_1$ (the third peak/the first peak in the emission spectra of pyrene in polymer solutions) intensity ratio vs logarithm of micelle concentration. Figure S4 shows the $I_3/I_1$−Log C plots for PEG-PPMT with 11%, 28%, 40%, 55% and 70% PDL contents. The copolymer CMC data calculated from the plots are summarized in Table S1.

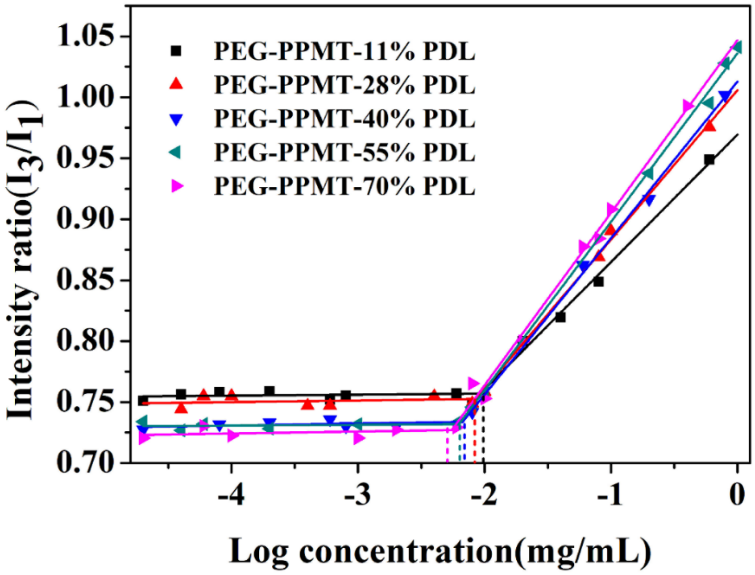


**Figure S4**. $I_3/I_1$ ratio as a function of logarithm of polymer concentration (Log C) of PEG-PPMT copolymers in PBS solution (10 mM, pH 7.4).

**Table S1**. CMC data of PEG-PPMT block copolymers.

| Sample | CMC(μg/mL) |
|---|---|
| PEG-PPMT-11%PDL | 9.96 |
| PEG-PPMT-28%PDL | 8.57 |
| PEG-PPMT-40%PDL | 6.71 |
| PEG-PPMT-55%PDL | 6.29 |
| PEG-PPMT-70%PDL | 5.52 |

### 3. *In vitro* nanoparticle stability of PEG-PPMT copolymers

Solutions of PEG-PPMT nanoparticles in PBS (pH 7.4, 10 mM) containing 10% fetal bovine serum (FBS) were kept at 37 °C in a shaking bed with a rotation speed of 100 rpm, and were monitored periodically by DLS to measure the average nanoparticle size of the copolymers. The results shown in Figure S5 indicate that all PEG-PPMT nanoparticle samples remain fairly stable over the 7-day study period.

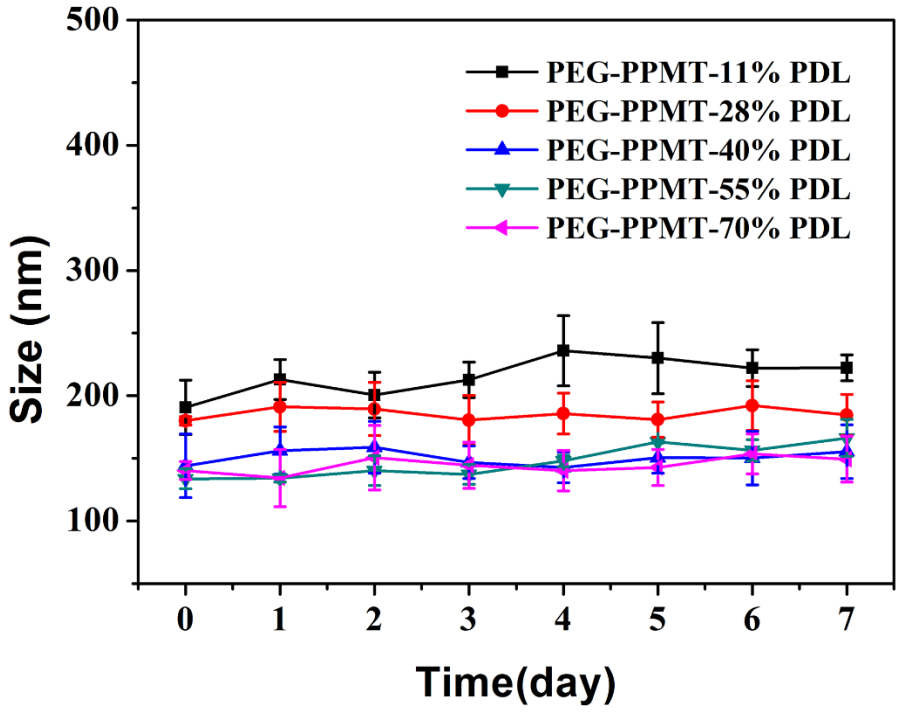


**Figure S5**. Average particle size vs incubation time for PEG-PPMT blank nanoparticles incubated in PBS (10 mM, pH 7.4) with 10% FBS. Data are given as the mean ± SD (n = 3).

**4. Cellular uptake under acidic pH**

CT-26 cells were incubated in culture media with pH of 6.5 containing C6-loaded PEG-PPMT-11% PDL nanoparticles or C6-loaded PEG-PPMT-28% PDL nanoparticles (yielding final C6 concentration at 0.2 μg/mL) for 1-8 h. After trypsinized and resuspended, the cells were detected by FACS Calibur flow cytometer to quantify the cellular internalization efficiency of the nanoparticles. FlowJo software was used for data analysis and all flow cytometry data shown were initially gated on live cells.

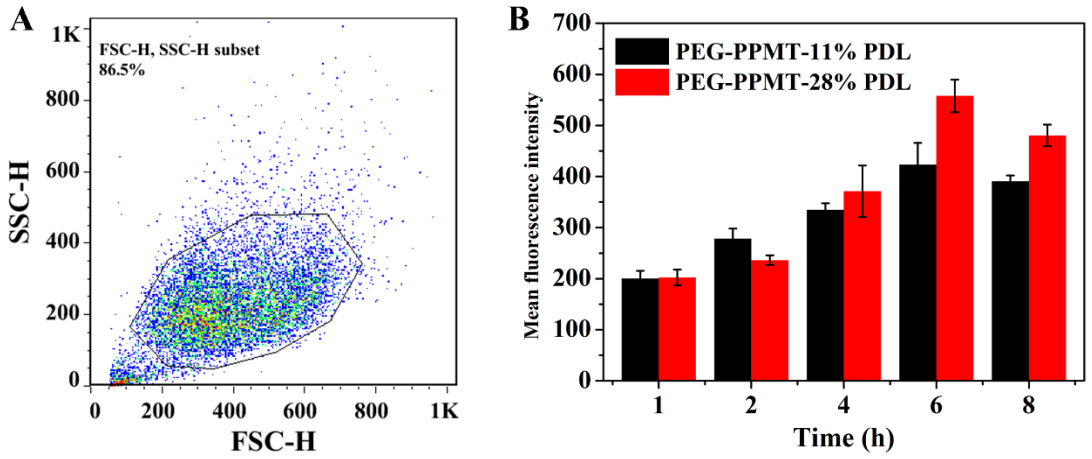


**Figure S6**. (A) Gating strategies for the flow cytometry analyses; (B) Flow cytometry analysis of the CT-26 cells incubated in culture media with pH of 6.5 containing different C6-loaded PEG-PPMT nanoparticles. Data are given as mean ± SD (n = 3).

**5. Abundance of ROS components in tumor cells**

Intracellular ROS components were detected using DCFH-DA Reactive Oxygen Species Assay Kit. As one of the most general and sensitive fluorescence probes for quantification of intracellular ROS, non-fluorescent 2′,7′-dichlorofluorescein diacetate (DCFH-DA) is converted to fluorescent dichlorofluorescein (DCF) after cellular uptake, and the fluorescence intensity of DCF is indicative of intracellular ROS level.

For quantitative evaluation of intracellular ROS levels, HeLa, HepG2, SW620 and CT-26 cells were plated onto 24-well plates at a density of $2 \times 10^5$ cells/well and cultured for 24 h at 37 °C under an atmosphere of 5% $CO_2$. Thereafter, fresh medium containing DCFH-DA (10 μM) was added, followed by further incubation for 20 min. The intracellular ROS levels were determined by measuring DCF fluorescence intensity using flow cytometric examination at an excitation wavelength of 504 nm and an emission wavelength of 525 nm. The relative intracellular ROS abundances obtained for the four different cancer cell lines (HeLa, HepG2, SW620 and CT-26 cells) are displayed in Figure S7. All cell lines exhibit an elevated ROS content, and it is also observable that intracellular ROS abundance can vary substantially among different cancer cell lines.

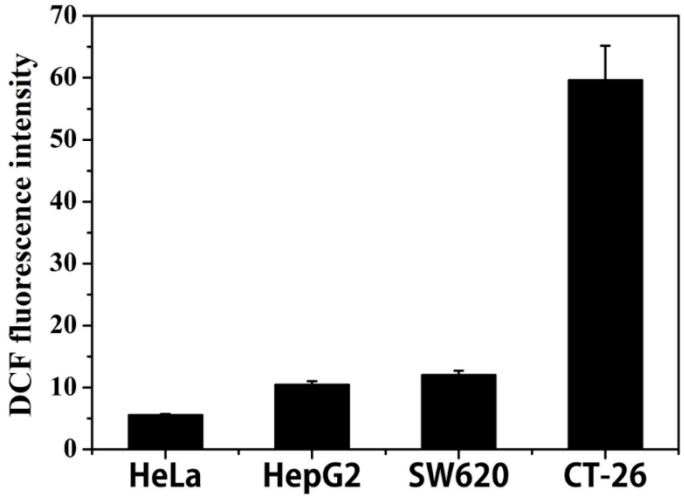


**Figure S7**. Quantitative analysis of intracellular ROS level in HeLa, HepG2, SW620 and CT-26 cell lines.

## 6. Cytotoxicity of blank PEG-PPMT nanoparticles

CT-26 and HeLa cells were treated with blank PEG-PPMT nanoparticles in the media at 37 °C for 48 h. The viabilities of the cell groups at different nanoparticle concentrations were measured by MTT assay (Figure S8). The results show that the PEG-PPMT nanoparticles are essentially nontoxic at concentrations up to 400 μg/mL.

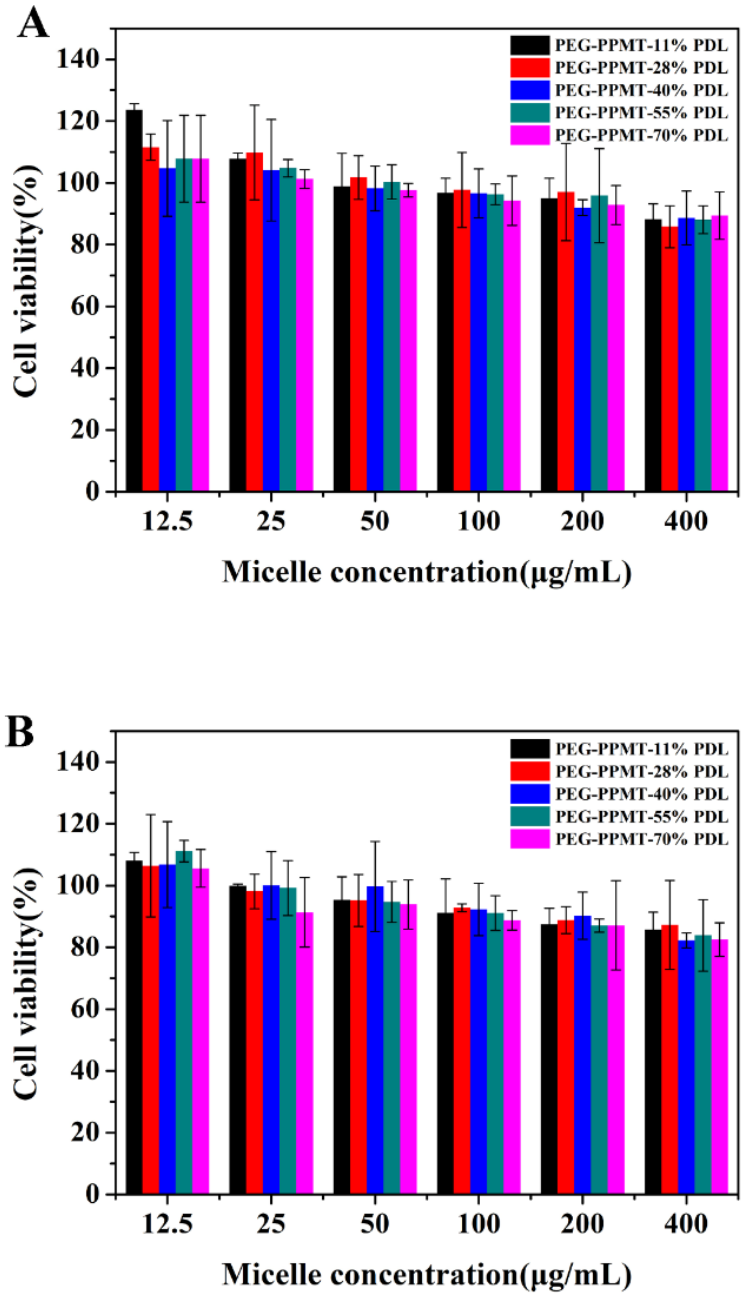


**Figure S8**. Viabilities of (A) CT-26 cells and (B) HeLa cells after incubation at 37 °C for 48 h with various amounts of PEG-PPMT blank nanoparticles. Data are given as mean ± SD (n = 3).

**Table S2.** The $IC_{50}$ value of different DTX-loaded nanoparticles and free DTX against CT-26 cells and HeLa cells under different pH.

| Cell line | pH | PEG-PPMT-11% PDL | PEG-PPMT-28% PDL | PEG-PPMT-40% PDL | PEG-PPMT-55% PDL | PEG-PPMT-70% PDL | Free DTX |
|---|---|---|---|---|---|---|---|
| CT-26 | 7.4 | 0.491 | 0.688 | 0.713 | 1.293 | 7.146 | 10.049 |
| | 6.5 | 0.024 | 0.084 | 0.306 | 0.677 | 1.678 | 9.442 |
| HeLa | 7.4 | 0.253 | 0.348 | 0.330 | 2.354 | 10.289 | 15.391 |
| | 6.5 | 0.111 | 0.241 | 0.212 | 2.022 | 9.270 | 13.740 |

## 6. Erythrocyte agglutination and hemolysis assay

The PEG-PPMT nanoparticles were incubated with erythrocytes (RBCs) to determine blood compatibility of the copolymers. The blank nanoparticles (50 to 500 μg/mL) and $1 \times 10^8$ RBCs were mixed in PBS and the mixtures were then incubated for 2 h at 37 °C. Subsequently, the samples were centrifuged for 10 min at 1000 rpm and the supernatants were analyzed by a microplate reader to measure their absorbance at 413 nm. During the hemolysis assay, Triton-100 (1%, w/v) and isotonic PBS were tested as positive and negative controls, respectively. Hemolysis value was calculated by following equation:

$$\text{Hemolysis}\,(\%) = \frac{A_{sample} - A_{PBS}}{A_{Triton} - A_{PBS}} \times 100\%$$

where $A_{Sample}$, $A_{PBS}$, and $A_{Triton}$ represent the absorbance intensity values of the supernatants from RBCs treated with the nanoparticle samples, PBS and Triton X-100, correspondingly. All PEG-PPMT nanoparticle samples exhibit minimal hemolytic activity at polymer concentrations up to 500 μg/mL (Figure S9). Consistently, microscopic images of erythrocytes ($1 \times 10^7$ RBCs/mL) after 2-h incubation with the nanoparticles show no agglutination of the erythrocytes (Figure S10).

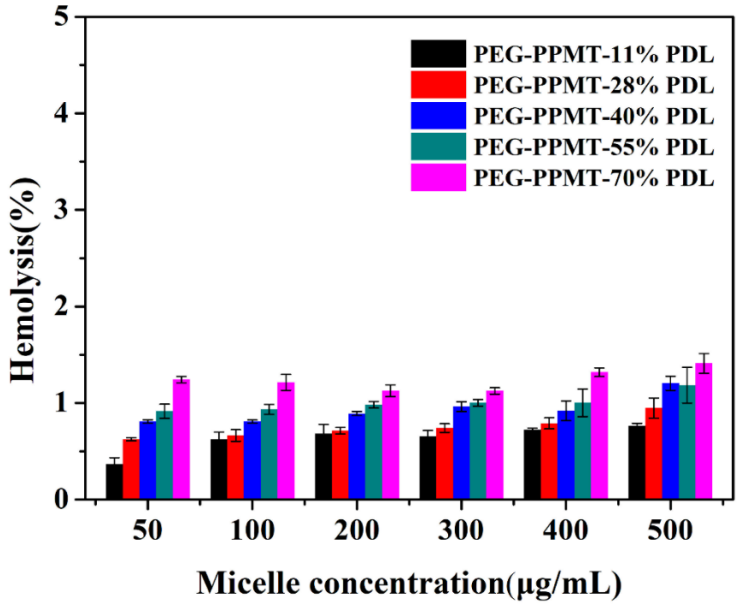


**Figure S9**. Hemolytic activity of PEG-PPMT nanoparticles at different nanoparticle concentrations. Data are given as mean ± SD (n = 3).

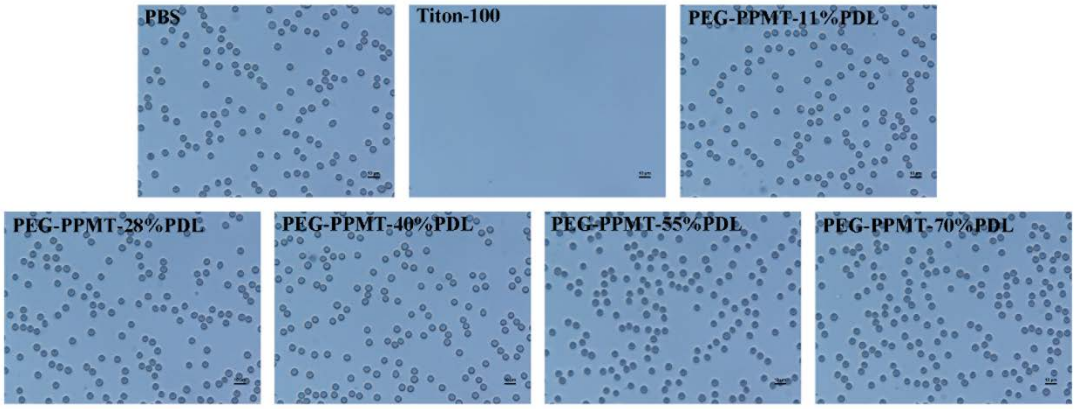


**Figure S10**. Microscopic images of erythrocytes after incubation with different blank PEG-PPMT nanoparticles for 2 h. Triton X-100 and PBS were used as the positive and negative controls, respectively.

## References

S1 B. Liu, X. Zhang, Y. Chen,Z. Yao, Z. Yang,D. Gao, Q. Jiang, J. Liu and Z. Jiang, *Polym. Chem*. 2015, **6**, 1997.